JOURNAL OF THE AMERICAN WATER RESOURCES ASSOCIATION
FEBRUARY AMERICAN WATER RESOURCES ASSOCIATION 2004

PREDICTION OF STREAM TEMPERATURE IN FORESTED WATERSHEDS[1]

V. Sridhar, Amy L. Sansone, Jonathan LaMarche, Tony Dubin, and Dennis P. Lettenmaier[2]

ABSTRACT: Removal of streamside vegetation changes the energy balance of a stream, and hence its temperature. A common approach to mitigating the effects of logging on stream temperature is to require establishment of buffer zones along stream corridors. A simple energy balance model is described for prediction of stream temperature in forested headwater watersheds that allows evaluation of the performance of such measures. The model is designed for application to "worst case" or maximum annual stream temperature, under low flow conditions with maximum annual solar radiation and air temperature. Low flows are estimated via a regional regression equation with independent variables readily accessible from GIS databases. Testing of the energy balance model was performed using field data for mostly forested basins on both the west and east slopes of the Cascade Mountains, and was then evaluated using the regional equations for low flow and observed maximum reach temperatures in three different east slope Cascades catchments. A series of sensitivity analyses showed that increasing the buffer width beyond 30 meters did not significantly decrease stream temperatures, and that other vegetation parameters such as leaf area index, average tree height, and to a lesser extent streamside vegetation buffer width, more strongly affected maximum stream temperatures.
(KEY TERMS: stream temperature prediction; watershed management; best management practices; GIS; water quality; stream energy balance.)

Sridhar, V., Amy L. Sansone, Jonathan LaMarche, Tony Dubin, and Dennis P. Lettenmaier, 2004. Prediction of Stream Temperature in Forested Watersheds. Journal of the American Water Resources Association (JAWRA) 40(1):197-213.

INTRODUCTION

Water quality changes associated with timber harvesting have been a concern of environmental planners and regulators at least since the 1960s (Salo and Cundy, 1987). Logging of near stream vegetation affects water temperature primarily by altering solar radiation incident on the stream, and hence the balance of net radiation, turbulent heat exchange across the water surface boundary, stream/streambed heat exchange, and advection of heat via ground water and the net flux across the reach boundaries. Elevated stream temperatures affect all aspects of the aquatic environment including the type and abundance of primary producers, the life stage cycles of benthic invertebrates and fishes and the chemical composition of the water (Hynes, 1970).

The Washington State Joint Natural Resources Cabinet (WSJNRC, 1999, unpublished report) found that elevated temperatures were the second major cause (after bacteria) of Washington streams not meeting Water Quality Standards under the federal Clean Water Act of 1972 and that water temperature, the level of dissolved oxygen, and acidity were critical factors for salmon spawning and rearing. Forests cover almost half of the State of Washington and most of the salmon bearing streams have their headwaters in forested regions (WSJNRC, 1999, unpublished report). Nineteen Washington salmon, steelhead, and trout fish populations have been listed under the Endangered Species Act (ESA) as threatened or endangered since 1992. A critical aspect of the development of recovery plans under ESA is the requirement for accurate prediction of stream temperature changes due to logging. Sixty-seven percent of the forest lands in the State of Washington are now covered with young trees due to logging over the past 30 years. To address the issue of changed (generally elevated) stream temperatures following logging, "best management practices" (BMPs) have been

[1]Paper No. 02131 of the *Journal of the American Water Resources Association* (JAWRA) (Copyright © 2004). **Discussions are open until August 1, 2004.**
[2]Department of Civil and Environmental Engineering, University of Washington, Seattle, Washington 98195 (currently: Sansone at Three Tier, 2825 Eastlake Avenue East, Seattle, Washington 98102; LaMarche at Oregon Water Resources Department, Bend, Oregon 97701; and Dubin at Brown and Caldwell, Seattle, Washington 97701) (E-Mail/Lettenmaier: dennisl@u.washington.edu).

implemented in states with silviculture activities under the Clean Water Act. The BMP most often implemented is to leave a fixed width "buffer zone" along the stream within which the vegetation is not disturbed by logging (Rishell *et al.,* 1982; Brosofske *et al.,* 1997).

Computer models can be an effective tool for predicting stream temperatures and evaluating the effectiveness of BMPs. Various physically based models have been developed for modeling temperature in small mountain streams (Theurer, 1984; Sullivan *et al.,* 1990). Initially, water temperature models were developed to predict temperature changes in large rivers and lakes due to dams and heated effluent discharges (Jaske, 1965; Brown, 1969; Sartoris, 1976). These applications contrast with those of interest to forest managers, which are usually small streams in forested mountainous regions. To predict stream temperatures accurately in such environments, models are needed that take into account both topographic and vegetation effects on the energy balance. Different components of the energy balance are important when modeling small streams as opposed to large rivers. Ground water advection, for instance, is often ignored when modeling large rivers but may be significant for small streams under low flow conditions (Brown, 1969). On the other hand, complete lateral and depth mixing (one-dimensional assumption) is often an appropriate assumption for small headwater streams, whereas in large rivers vertical temperature gradients are often significant (Hynes, 1970).

Though there are many stream temperature models available (Andradóttir and Nepf, 2000; Lowney, 2000) many, if not most, tend to focus on the hydraulic aspects of the problem, and less so on estimation of the radiant forcings and the environmental management factors (e.g., streamside vegetation) that influence them. This paper describes a stream temperature model that, while based on physical principles, is easily implemented using data commonly available from geographic information system (GIS) databases, and that is focused on prediction of maximum stream temperatures during the critical summer low flow period. In this work, the basis is provided for a physically based representation of vegetation, and its interaction with stream geometry and topography, as well as vegetation, as it affects the (dominant) radiative forcings. Also included (as hydraulic models generally do not) are methods of obtaining, in a consistent manner over a landscape, the temperature forcings, as well as the seven-day, 10-year low flow regime (7Q10), which are estimated via regional regression. The model is designed to replace empirical approaches like the Sullivan *et al.* (1990) algorithm currently incorporated in the Washington Forest Practices Manual. The motivation for development of the model is twofold. The first is to provide the basis for determining a potential maximum stream temperature based on 7Q10 flow regimes and 10-year maximum air temperature. The second is to allow a basis for exploring the effects of alternative streamside vegetation management strategies on the potential maximum stream temperature. The model is simple enough to be used in forest management and planning applications.

BACKGROUND

The energy balance of a control volume (e.g., stream reach) is the sum of the net heat flux (advection and diffusion) through the volume plus sources less sinks (Chapra, 1997). For upland streams, a one-dimensional simplification of the more general three-dimensional energy balance equation is appropriate, as given in Equation (1). In Equation (1), Q is stream discharge, x is longitudinal distance, T is water temperature, D_L is the longitudinal dispersion coefficient, A is the stream cross sectional area (of an assumed rectangular channel), d is the stream depth, ρ is the density of water, and E is the net of heat sources and sinks (energy fluxes to or from) the reach. For Equation (1) to apply, the system is assumed to be well mixed laterally and vertically, and hence transverse and vertical diffusivity are assumed to be small. Furthermore, longitudinal dispersion is assumed to be much larger than the turbulent diffusivity. In other words, the assumption that longitudinal dispersion is much larger than the turbulent diffusivity results in a simplified one-dimensional, advection/dispersion equation that can be used for relatively steep upland streams. It should be noted that longitudinal dispersion exists in well mixed systems whether or not the velocity is constant.

$$A\frac{\partial T}{\partial t}+\frac{\partial (QT)}{\partial x}=\frac{\partial}{\partial x}\left[AD_L\frac{\partial T}{\partial x}\right]+\frac{EA}{\rho C_p d} \tag{1}$$

For a constant cross section and flow, Q/A is the mean reach velocity V, and Equation (1) reduces to

$$\frac{\partial T}{\partial t}+V\frac{\partial T}{\partial x}=D_L\frac{\partial^2 T}{\partial x^2}+\frac{E}{\rho C_p d} \tag{2}$$

which is the basis for the model described in this paper. Solution of Equation (2) is straightforward, but determining the reach energy flux, E, requires understanding the interaction of the stream reach with the streamside environment, especially as it affects solar

radiation, which is the dominant energy flux term under the maximum annual stream temperature scenarios evaluated.

The heat transfer between the stream and its surrounding environment is composed of the net heat exchange between the water and the atmosphere and the net heat exchange between the water and the streambed. The heat exchange between the air and the stream is governed by four main processes: heat input from (net) solar radiation, heat loss/gain from longwave radiation, heat loss due to evaporation (latent heat), and convection of heat across the air-water interface (sensible heat). The heat exchange between the streambed and the stream (which are neglected for reasons indicated below) is governed by heat loss/gain from conduction.

Solar radiation incident on the stream surface can be strongly affected by streamside vegetation, and topography. Surface solar radiation has a strong diurnal cycle, whereas longwave radiation is relatively constant over a day. However, upward longwave radiation is an important term in the stream reach energy balance under clear sky conditions, which are present during the "worst case" summer condition of maximum stream temperature. Both evaporation, which results in the loss of heat from the evaporative surface, and convection (sensible heat) across the air/water interface can be computed using bulk aerodynamic equations in which the potential is the saturation vapor pressure deficit in the case of latent heat, and the stream surface temperature – air temperature difference in the case of sensible heat. These terms are therefore linked by the Bowen ratio (Bowen, 1926), and both depend on the stream surface temperature (to which the saturation vapor pressure is related in the case of latent heat). Heat conduction is neglected between the water and the streambed as the computed transfer rates given typical thermal conductivities for saturated soils, and the temperature differential between maximum stream temperature and annual average air temperature (usually a good surrogate for soil temperatures) is much smaller than net radiation. The authors recognize, though, that in some cases (especially streams with rocky bottoms), this term can be important (Brown, 1969).

Many stream temperature models have been developed that make various simplifying assumptions – often the one-dimensional assumption is made, and in some cases, steady flow as well. The intent is not to improve on these models, but rather to focus on the source and sink (net energy flux) term, which is directly related to environmental conditions, especially streamside vegetation, in the case of forested upland streams. It is noted that the existing models have sometimes been difficult to apply in practice. Sullivan *et al.* (1990), for instance, found that all of the "standard" models evaluated were either too complex, needed data that were not readily available, or did not predict stream temperatures accurately. The objective here is to develop a simple model, applicable specifically to "worst case" conditions, that utilizes data that can be readily extracted from commonly available GIS data bases.

DEVELOPMENT OF GIS STRTEMP MODEL

Low Flow Prediction

A critical term in Equation (1) is the discharge, Q (to which the mean reach velocity, V, in Equation (2) is related). One difficulty in application of physically based stream temperature models is that discharge is not usually available from observations except for the relatively small number of reaches that are gauged. Furthermore, the upstream drainage area of gauged reaches often is larger than that draining to reaches of management interest in forested watershed. Therefore, as the first step in the model development, regional regression equations were developed based on low flow discharge observations at stream gages that could then be transferred to ungauged reaches. In this work, the reference discharge used was the 7Q10 seven-day, 10-year low flow, although the method could be applied to other discharges as well. The regional regression equations were of a general form that has long been used by the U.S. Geological Survey (USGS) (see, e.g., Thomas and Benson, 1970). One consideration in selection of candidate basin characteristics was that they should be extractable from readily available GIS databases (e.g., mean annual precipitation, drainage area, channel slope and aspect, and other characteristics that are derivable from digital topographic data, vegetation characteristics, and similar attributes). The candidate characteristics that were evaluated included drainage area, average annual precipitation, total channel length upstream of the reach, main channel slope, and gage station elevation. Multiple linear regression models were developed to relate 7Q10 to these attributes. Also, relationships were developed using the generalized least squares (GLS) method as described by Tasker and Stedinger (1989).

The average annual and monthly precipitation values for the reference period (1961 to 1990) were obtained from a 4 km (horizontal resolution) dataset, produced using the Parameter Elevation Regressions on Independent Slopes Model (PRISM) as described by Daly *et al.* (1994). The data were provided courtesy

of the Oregon Climate Service. Basin average precipitation was obtained by overlaying the PRISM precipitation and delineated catchment boundaries derived from 1 arc-second (approximately 30 m) digital topographic data. The length of the main channel and elevation of the upstream and downstream termini of the main channels were obtained from the 30 meter digital elevation model (DEM) and the national hydrography datasets (NHD) (courtesy of the USGS), from which an average main channel slope was extracted.

The regional regression model was intended for use within the region(s) for which the parameters were estimated, and (at least roughly) within the ranges of the predictor attributes. Therefore, applicability was restricted to perennial streams with drainage areas less than about 1500 km^2, and initially separate models were estimated for the east and west slopes of the Cascade Mountains. The "training" dataset for the regional regression models included 50 stations on the west side of the Cascade Mountains and 12 on the east side. Based on preliminary testing, and considering the small number of east side stations, a single model was estimated for the pooled data, and it was diagnosed separately for east and west side streams. The GLS method was chosen instead of the more commonly used ordinary least squares (OLS) method (Helsel and Hirsch, 1992) as two assumptions of the OLS method (i.e., variance of the residuals, ε, is constant and the residuals are independent) were likely to be violated.

The GLS regression analysis was performed using the USGS Generalized Least Squares Network Analysis (GLSNET) software, which is based on estimation techniques developed by Stedinger and Tasker (1985) and Tasker and Stedinger (1989). GLSNET was used to calculate the 7Q10 low flow from the seven-day low flow for each station, which was estimated from long term station data through use of a Log Pearson Type III distribution.

The initial candidate explanatory variables were latitude, longitude, drainage area, average annual precipitation over the catchment, main channel slope, average basin elevation and total length. Parameters were eliminated using the t-test, PRESS (Prediction Error Sum of Squares) statistic and adjusted R^2 value (Helsel and Hirsch, 1992). The detailed description of variable selection and analysis to derive the final model can be found in Sansone and Lettenmaier (2001). The model with drainage area and precipitation as explanatory variables was found to be the best among those considered for prediction of 7Q10. The form and parameters of the estimated model are

$$\log10(7Q10_{flow}) = 1.4157 + 1.06257(\log10(area)) + 0.95125(\log10(precip)) \quad (3)$$

In the above equation, drainage area is in square miles, precipitation is in cm, and the flow is in cfs. The applicability of the regression model was verified for basins located on both the east and west sides of the Cascades by plotting the predicted 7Q10 low flow against the residuals to determine if any trends existed in the variance that would indicate that the west and east side data could not be pooled (Figure 1). The analysis showed that a single model is adequate (the primary reason is that precipitation, which is generally lower for east side streams at the same elevation, acts as a surrogate for location). The expected behavior of low flows in forested catchments in the Cascades is that flow increases with higher precipitation and larger drainage areas. However, drainage areas of the stations analyzed tend to decrease and precipitation tends to increase as elevation increases.

Energy Balance

The reach energy balance model is based on a finite difference approximation to the one-dimensional, steady state, reach energy balance equation (Equation 2), where the reach length, L, is discretized into n subreaches, resulting in

$$\frac{T_i^{t+1} - T_i^t}{\Delta t} + V\frac{T_{i+1}^t - T_{i-1}^t}{2\Delta x} = D_L\frac{T_{i+1}^t - 2T_i^t + T_{i-1}^t}{\Delta x^2} + \frac{E_i^{t+1} + E_i^t}{2\rho c_p d} \quad (4)$$

Solving in terms of temperature at time t+1 for node i gives

$$T_i^{t+1} = T_i^t = \Delta t\, V\frac{T_{i+1}^t - T_{i-1}^t}{2\Delta x} + \Delta t\, D_L\frac{T_{i+1}^t - 2T_i^t + T_{i-1}^t}{\Delta x^2} + \Delta t\frac{E_i^{t+1} + E_i^t}{2\rho c_p d} \quad (5)$$

If the stream is well mixed, D_L can be estimated as $D_L = 0.5\ V\Delta x$ (Sinokrat and Stefan, 1993). The energy term at time t + 1 (E_i^{t+1}) contains components that are dependent on water temperature at the same time step. Therefore, an iterative approach is used in conjunction with the finite difference equation to account for this dependence in the solution. The method consists of initially assuming $T_i^{t+1} = T_i^t$, and computing the energy term, E_i^{t+1}. Subsequently, the finite difference equation is solved giving a new value of T_i^{t+1}. The last two processes are repeated until the difference between the initial and new T_i^{t+1} value is negligible. The convergence criterion used was $\Delta T \leq 10^{-5}$°C.

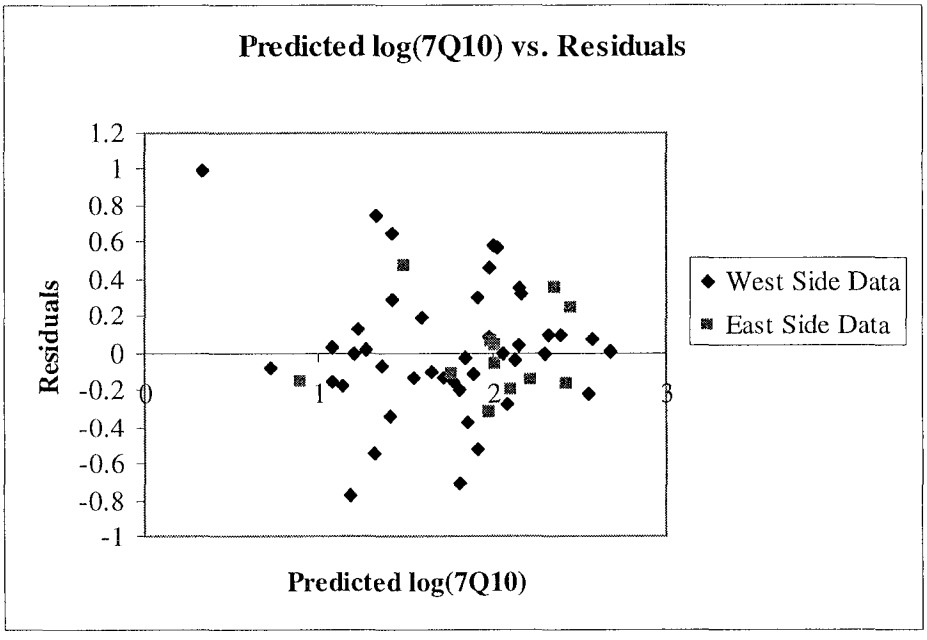

Figure 1. Plot of the Predicted log(7Q10 discharge) Versus the Residuals for Basins Located on Both the East and West Sides of the Cascades.

The model is formulated so that the user selects a stream reach of interest and extracts pertinent information such as drainage area, stream azimuth, slope, and aspect that are extracted from the GIS databases for input into the stream energy balance submodel. The user also specifies parameters related to streamside vegetation such as the streamside canopy and trunk heights, bank to canopy distance, buffer width, and leaf area index (LAI). The initial water temperature, which is one of the model inputs, corresponds to the temperature at the upstream boundary of the reach. Through sensitivity testing it was found that a stream reach greater than about 1,800 m was needed to eliminate the influence of the initial starting temperature on the predicted water temperature. To avoid this problem, a buffer reach of 3,000 m was specified ending at the upstream boundary of the reach of interest, for which the downstream most temperature was used to represent the upstream boundary initial water temperature in the computational domain – that is, the water temperature simulated at the end of the buffer reach was used as the initial water temperature for the stream reach of interest.

The energy exchange, E, between the stream and its environment is a function of incoming and reflected short wave radiation, incoming long wave radiation from the sky and riparian canopy; emitted long wave radiation from the stream, and convective heat exchange between water and air; and evaporation and condensation between the air/stream interface and advection from ground water gains or losses. The formulations used in the model for net long and short wave radiation, advection, and latent and sensible heat are summarized briefly below. For details, the reader is referred to Sansone and Lettenmaier (2001).

Solar Radiation. Direct and diffuse beam solar radiation are calculated at user defined spatial and temporal intervals along the stream reach of interest using a version of the Solarflux add-on for ARC/INFO (Dubayah and Rich, 1995; Rich *et al.,* 1994), which has been modified to include the shading effects of near stream vegetation.

Direct Solar Radiation – Direct beam solar radiation incident on the top of the vegetation canopy (or on the stream surface if the sky view is not obstructed by vegetation) is given by

$$I_{direct} = \tau S_o[\sin(\alpha)\cos(\varphi)\cos(\theta_{sun} - \beta)+\cos(\alpha)\sin(\varphi)] \quad (6)$$

where τ is atmospheric transmissivity, S_o is the solar constant, α is the angle of the earth's surface from a horizontal plane, φ is solar illumination angle above the horizon, θ_{sun} is the angle of sun relative to north (solar aspect), and β is the downslope direction of the maximum rate of change in elevation relative to north.

Diffuse Solar Radiation – It is assumed that no diffuse radiation is transmitted through the forest canopy. For solar radiation directly incident on the stream surface, diffuse radiation is estimated using empirically derived equations given by Rich *et al.* (1994)

$$I_{diffuse} = f \times S_o[0.271 - 0.294\tau]\frac{1+\cos(\alpha)}{2\sin(\varphi)} \quad (7)$$

where f is the sky view factor (i.e., the fraction of the hemispheric view upwards from the center of the stream that is open to the sky, which varies from 1.0 (unobstructed) to 0.0 (completely obstructed).

Forest Effects on Direct Solar Radiation. Direct beam shortwave radiation can either be incident directly on the stream surface, or it can be transmitted through (and attenuated by) the canopy and subsequently reach the stream surface. The first pathway is dominant when the orientation of the stream is close to the azimuthal angle of the sun, or if the stream is wide, or if the vegetation is short or sparsely distributed.

The second pathway is more common for smaller (lower order) streams with dense vegetation cover. To describe the attenuation of light through the vegetative canopy, it is further partitioned into fractions F2 and F3 as shown in Figure 2 depending on how much of the canopy the beam passes through before reaching the stream surface. The attenuation of beam radiation fractions F2 and F3 is estimated using Beer's law (Monteith and Unsworth, 1990)

$$I_{direct} = I_o \times \exp(-k.LAI) \quad (8)$$

where I_o is the above canopy direct beam radiation (computed by Equation 6); k is the coefficient of attenuation (which is a function of the path length through the canopy, and hence is different for F1, F2, and F3, and depends also on the solar angle); and *LAI* is the leaf area index. The leaves are assumed to be perfect (black) radiators, which has the effect of ignoring scattering within the canopy. In the modified SOLARFLUX model, k varies from 0.2 to 0.5 depending on the path length of light through the canopy. For small buffers (noted as F3) with path lengths at low angles, a value of k between 0.1 and 0.35 is used. First, the attenuation of beam radiation fraction F1 is computed as

$$F1 = 1 - \left(X + BC/W_{stream}\right) \quad (9)$$

where W_{stream} is the stream width, BC is the bank canopy distance,

$$X = Ht_{Tree} \times \left(\left|\frac{\sin(\theta sun - \theta stream}{\tan\varphi}\right|\right), \quad (10)$$

and Ht_{Tree} is the tree height. If X < BC, F1 =1 and if X > W_{stream} + BC, F1 = 0. When F1 < 1, F2 is computed as the ratio of bank width to stream width. If F1 = 0, then F2 is computed as

$$F2 = \frac{BW - (X - W_{stream} - BC)}{W_{stream}} \quad (11)$$

where BW is the bank width. If F2 > 1, F2 = 1 and if F2 < 0, F2 = 0. Therefore, F3 = 1 - F1 - F2. Thus, direct beam solar radiation computed after partitioning is used as an input in the energy balance, finite difference module of the simulation.

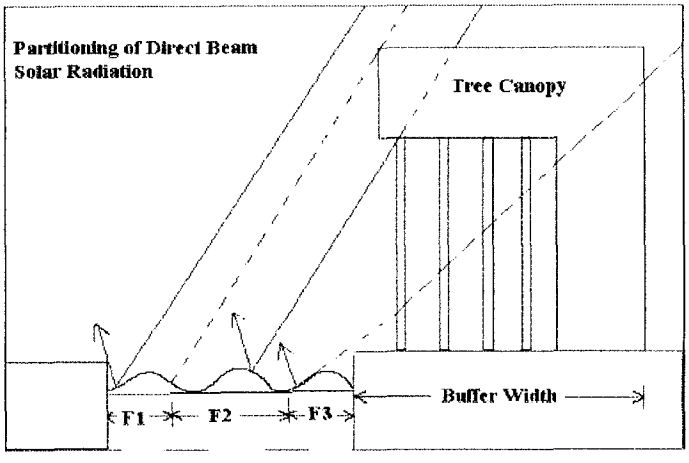

Figure 2. Vegetative Partitioning of Incoming Direct Beam Solar Radiation.

Long Wave Radiation. Downward long wave radiation is the sum of contributions from the air and the canopy (L_{air} and L_{tree}). Net long wave radiation therefore is given by

$$L_n = L_{air} + L_{tree} - L_{water} = \sigma\left[(e_a + e_t)T_a^4 - e_w T_w^4\right] \quad (12)$$

where σ is Stefan Boltzman constant, T_a is air temperature, T_w is water temperature, L_{water} is the emitted radiation by the water, e_w is the emissivity of water, e_a is the emissivity of air,

$$e_a = e_{ac}\,(1 + 0.17(CL^2)) \tag{13}$$

with e_{ac} the emissivity of air without cloud cover, taken from Shuttleworth (1993),

$$e_{ac} = 1 - 0.261\exp\left(-7.5\times10^{-5}\times T_a^4\right) \tag{14}$$

and CL is the percentage of cloud cover.

Advection. Advection, the heat gain or loss from ground water, is computed in the model as

$$A = \rho C_p Q_g (T_g - T_w) \tag{15}$$

where C_p is the specific heat of water, Q_g is the ground water flow into the reach, and T_g and T_w are the ground water and stream water temperatures, respectively. All flow under critical, low flow conditions is assumed to be derived from ground water; hence, the contribution for each reach is computed as the difference between the 7Q10 at the upstream and downstream reach boundaries. Also, ground water temperature variability is not considered because its effect on stream temperature is considerably less than the effects of atmospheric conditions (including net radiation). Various other studies (e.g., Sinokrat and Stefan, 1993; Lowney, 2000) have reported that ground water temperature variations tend to be small, both seasonally and diurnally, for depths more than a few meters. Based on some limited experiments where the ground water temperature was changed by up to 3°C, the change in stream temperature was less than 0.3°C. Furthermore, on a typical summer day, the ground heat flux component of the surface energy budget is less than 5 percent of the net radiation, suggesting that conduction between the stream and the stream bed is smaller than the other terms in the surface energy budget.

Latent Heat. Latent heat is based on the Penman equation (Penman, 1948) for potential evaporation from a shallow, free water surface (Shuttleworth, 1993).

$$E_p = \frac{\Delta}{\Delta+\gamma}\left(R_n + A_h\right) + \frac{\gamma}{\Delta+\gamma}\frac{6.43(1+.536U_2)\left[e_s(T) - e_a(T_a)\right]}{\lambda} \tag{16}$$

where Δ is the gradient of the saturation vapor pressure $e_s(T)$with respect to T, γ is psychrometric constant (kPa/°C), λ is the latent heat of vaporization of water (MJ/Kg), U_2 is wind speed at two meters (m/s), $e_s(T) - e_a(T_a)$ is the vapor pressure deficit of the air near the stream surface, (kPa), R_n is the net radiation at the free water surface, and A_h is advected energy.

Sensible Heat. The convective heat exchange across the air water interface is estimated by

$$C = 0.0124 \cdot U_2 \cdot P(T_w - T_a) \tag{17}$$

(Raphael, 1962) where P is atmospheric pressure (kPa), and T_w and T_a are the water and air temperatures (°C), respectively.

GIS STRTEMP MODEL EVALUATION

Model evaluation was performed in two steps. First, for the Entiat and Beckler Rivers, located east and west of the Cascades, respectively (Figure 3), stream temperature was measured continuously over a period of about two months during the summer of 2000, and model predictions were compared with observations. Subsequently, simulations were performed over a large area of the eastern Cascades including the Methow, Lake Chelan, Wenatchee, and Upper Yakima River basins for which sporadic measurements were available. The physiography, vegetation, and climate conditions of all six basins are summarized in Table 1. In general, east slope basins have warmer summer air temperatures, and lower annual precipitation, than do the west slope basins. Most of the drainage area of all of the basins is forested, although in some of the east slope basins the lower reaches have sparse vegetation. Within the forested areas, varying amounts of vegetation disturbance due to fire and logging have affected the streamside vegetation, and these effects are captured in the GIS vegetation data sets used in the modeling.

Entiat and Beckler Rivers Evaluation

Stream and air temperature data were collected in the Entiat and Beckler basins at hourly intervals from the end of July to the end of September 2000 using Hobo StowAway TidBit™ data loggers from the Onset Computer Corporation. The data loggers operate in the temperature range of -20°C to +50°C and have an accuracy of ±0.4°C. Point measurements of water temperature were also taken with a thermometer approximately weekly throughout the data collection period. The temperature loggers were placed at a minimum of three locations in each of the two

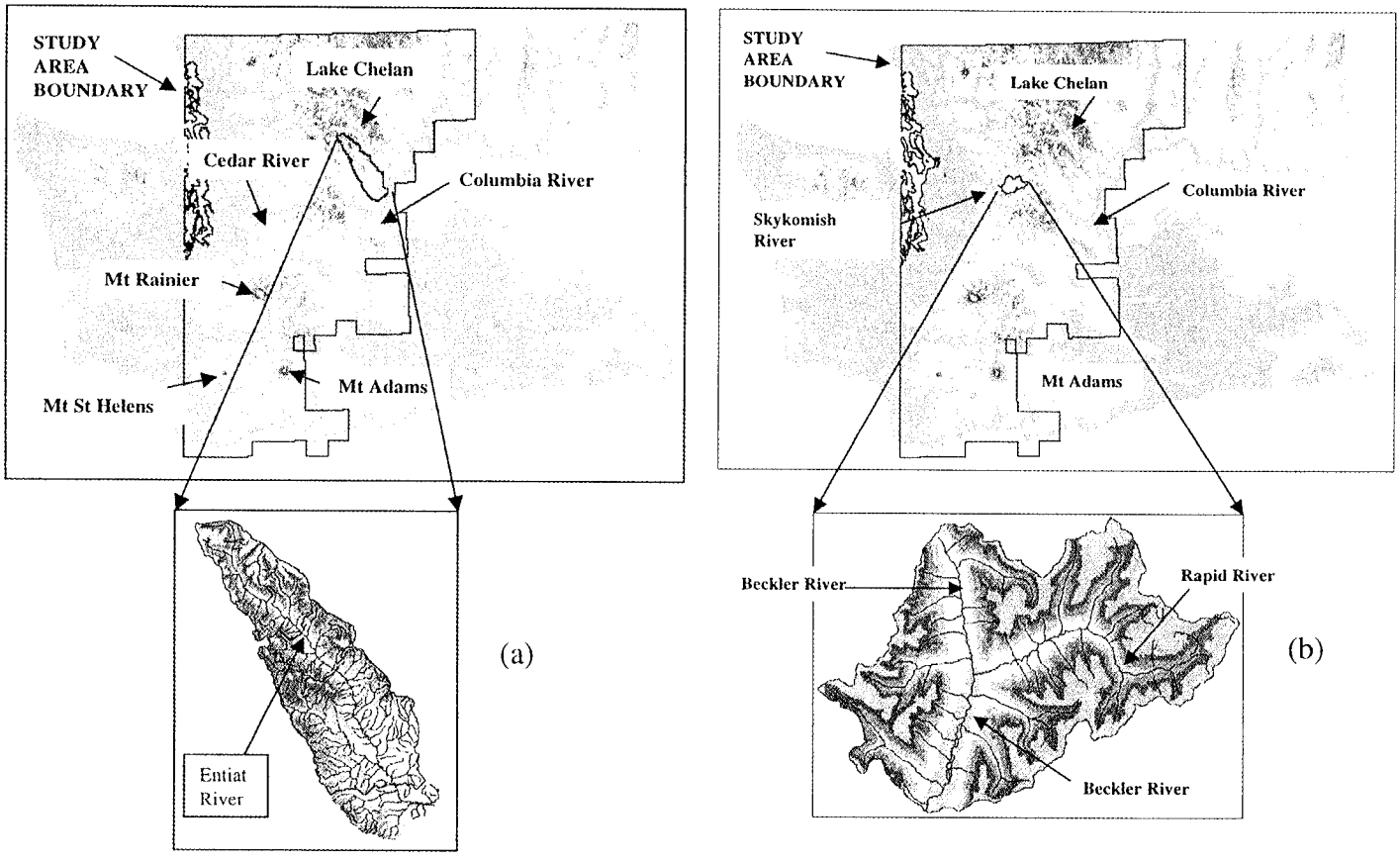

Figure 3. Location Map of the (a) Entiat and (b) Beckler River Basins.

TABLE 1. Characteristics of River Basins Used for Model Evaluation.

Basin	Drainage Area (km2)	Annual Precipitation (mm)		Streamside Vegetation
		Maximum	Minimum	
Entiat	907	2,300	250	Coniferous forest above river Km 30, shrub/steppe downstream
Beckler	260	2,700	2,100	Coniferous forest
Methow	4,600	2,000	1,500	Coniferous forest in upper reaches, shrub/steppe downstream
Chelan	2,700	3,800	250	Coniferous forest except shrub/steppe in lower reaches of downstream tributaries
Wenatchee	3,550	1,000	200	Coniferous forest above river Km 30, shrub/steppe downstream
Upper Yakima	5,500	2,300	150	Coniferous forest in upper reaches, shrub/steppe downstream

streams. In addition, one logger was placed at the most upstream and most downstream sites in each basin to record air temperatures. The loggers were attached to the bank using plastic coated clothesline wire. Protective casings were not used. The wire was placed under rocks on the bottom of the channel to ensure it would remain in place. The wire allowed the loggers to remain suspended in the water column above the streambed. Hourly data were collected continuously from the end of July through the middle of September. The air temperature loggers were placed on the banks of the stream out of direct sunlight, approximately 1.5 to 3.0 m (5 to 10 ft) from the water's edge. Two temperature loggers were placed at

each site to assure that data would be recorded even in the event of failure of one of the recorders.

U.S. Forest Service (USFS) stream temperature data collected within the Entiat River basin during the summer of 2000 were provided courtesy of the USFS Entiat Ranger Station and were used for comparison purposes. One of the USFS stations in the Entiat River was at Cottonwood Campground near the location of the authors' most upstream measurement point. The differences between the USFS values and the authors' at this site were within the range of accuracy of the instrument of ±0.4°C. Point stream temperature measurements were also taken to verify the logger data. Ancillary streamflow and canopy architecture data were also collected at selected sites along the Entiat and Beckler Rivers.

The GIS-STRTEMP model was tested using the meteorological data collected within the Entiat and Beckler basins for the period July through September 2000. The results of the model evaluation are summarized for the maximum, minimum, and average predicted and observed temperature during the period of observations in Table 2. The predicted water temperature was within 2°C of observations for all locations except for the Beckler upstream site and the Entiat downstream site. Further evaluation was carried out for 14 stream reaches at which model predicted maximum temperatures were compared with maximum observed temperatures (from both the authors' data and USFS observations) over the summer 2000 field season (in the case of the University of Washington observations) and the summers of 1988, 1999, and 2000 for USFS locations. These results are summarized in Table 3. The predicted maximum 10-year stream temperatures exceeded the measured maximum temperatures by several degrees C except for the Deer Creek above DeForest site. Insufficient data were available to determine the reason for this anomaly.

Eastern Cascades Demonstration

From a practical standpoint, agreement of the model and observations to within about 2°C over a range of locations is about as good as one can expect given the various uncertainties in estimation of energy forcings, discharge, and other factors that affect stream temperature. One might reduce these uncertainties somewhat by focusing on improved observations of variables such as downward solar radiation at specific sites. It is recognized, however, that detailed data generally will not be available for practical applications, and instead the focus is on an approach that allows generalized application with data that are widely available. The viability of the approach is demonstrated with simulation results for two substantially different environments, the east and west slopes of the Cascade Mountains. In this analysis, 10 reaches were identified in each of the four basins shown in Figure 4 and control runs were performed by fixing vegetation related parameters, to assess the

TABLE 2. Simulation Results of Entiat and Beckler River Basins.

	Measured and Predicted Daily Stream Temperatures (°C)					
	Average Daily		Minimum Daily		Maximum Daily	
Location	Measured	Predicted	Measured	Predicted	Measured	Predicted
Entiat – Upstream	8.4	9.9	6.8	8.2	9.8	11.0
Entiat – Midstream	9.7	10.5	8.1	8.9	11.5	11.6
Entiat – Downstream	11.3	12.3	9.2	10.8	13.7	13.4
Beckler – Upstream	9.3	10.6	8.1	9.3	10.6	11.6
Beckler – Midstream	12.2	12.7	10.8	11.2	13.8	13.9
Beckler – Downstream	13.5	13.3	11.7	12.3	15.8	14.1

	Average Differences (°C): Measured - Predicted		
Location	Average Daily Temperature	Minimum Daily Temperature	Maximum Daily Temperature
Entiat – Upstream	-1.5	-1.4	-1.1
Entiat – Midstream	-0.9	-0.8	-0.1
Entiat – Downstream	-1.1	-1.7	0.2
Beckler – Upstream	-1.3	-1.2	-0.9
Beckler – Midstream	-0.5	-0.3	0.0
Beckler – Downstream	0.2	-0.6	1.8

TABLE 3. Comparison of Predicted 10 Year Water Temperatures With Observed Maximum Summer Temperatures.

Stream Reach	Predicted Maximum 10-Year Water Temperature (°C)	Measured Maximum Water Temperature (°C)
Little Naches River	21.8	17.5
Crow Creek	23.3	16.0
Deer Creek Above DeForest	20.4	20.5
Mad River Above Pine Flat Campground	18.3	17.9
Hornet Creek	21.0	17.2
Preston Creek	19.8	17.2
Tillicum Creek	18.7	17.2
Entiat River at River Km 42	20.0	16.0
Entiat River – Upstream Field Site	16.9	12.0
Entiat River – Midstream Field Site	18.1	13.6
Entiat River – Downstream Field Site	20.1	16.0
Beckler River – Upstream Field Site	16.1	12.7
Beckler River – Midstream Field Site	18.4	16.0
Beckler River – Downstream Field Site	18.5	18.0

impact of changes in management practices on stream temperatures. The results are shown graphically in Figures 5 through 8 and the simulated minimum, maximum, and average temperatures are shown in Table 4. The 10-reach mean of maximum and average stream temperatures showed that the Chelan reaches had the lowest and the Methow reaches had the highest simulated stream temperatures (Figure 5). Similarly, mean minimum stream temperatures within the Lake Chelan basin were the lowest among all basins (Figure 6). The maximum temperatures simulated for the Methow basin range from 21.8°C in the headwater basin to 25.7°C in the most downstream basin. Low rainfall, and hence low baseflows per unit area, and semi-arid conditions in the lower altitudes of the basin with less dense vegetation contribute to the high maximum temperatures. Simulated maximum temperatures within the Wenatchee River basin (Figure 7: 22.3 to 25.1°C) and the upper Yakima River basin (Figure 8: 22.1 to 25°C) were quite similar.

Sensitivity Analysis

A sensitivity analysis was performed for a 1,500 m reach in the Entiat River basin to determine the effects of various controllable and uncontrollable model input parameters on predicted stream temperature. The analysis was carried out in standard fashion by varying one parameter while holding all others constant. That is, a set of values were prescribed for the parameters and subsequently those values were increased/decreased by certain a percentage arbitrarily. For instance, first the reference values are set for the parameters, tree height (20 m), LAI (7), bank/canopy distance (2 m) and buffer width (0 m) and then the incremental values for each of the parameters are used in the sensitivity analysis. The change in the predicted stream temperature was then determined for each parameter. The ranked sensitivity coefficients are shown in Table 5. It is important to note that some of the model parameters such as tree height and buffer width are correlated, and as in most such sensitivity analyses, some care must be exercised in interpreting the results.

One key result is that increasing the buffer width beyond 30 m did not significantly decrease stream temperatures in this stream reach. This result arguably could be an artifact of a short reach length, which might cause the upstream boundary condition to dominate the result. To explore this possibility, a range of stream reach lengths was tested varying from 0.5 km to 15 km. Over this variation in reach lengths, the change in stream temperature associated with changed buffer width ranged from 1.1 to 1.5°C, which indicates that the buffer width results were not controlled by the upstream boundary condition.

Other vegetation parameters that might be associated with land use management, such as average tree height, LAI, and bank/canopy distance more strongly affected stream temperatures, as shown in Table 5. Therefore, typical reaches were chosen within the Methow, Lake Chelan, Wenatchee, and Upper Yakima basins for additional sensitivity analyses. The parameters were fixed at nominal values, and incremental changes were applied to those parameters that might be affected by land use management: tree height, LAI, buffer width, and bank-canopy distance. The relative and absolute sensitivities were computed for each of

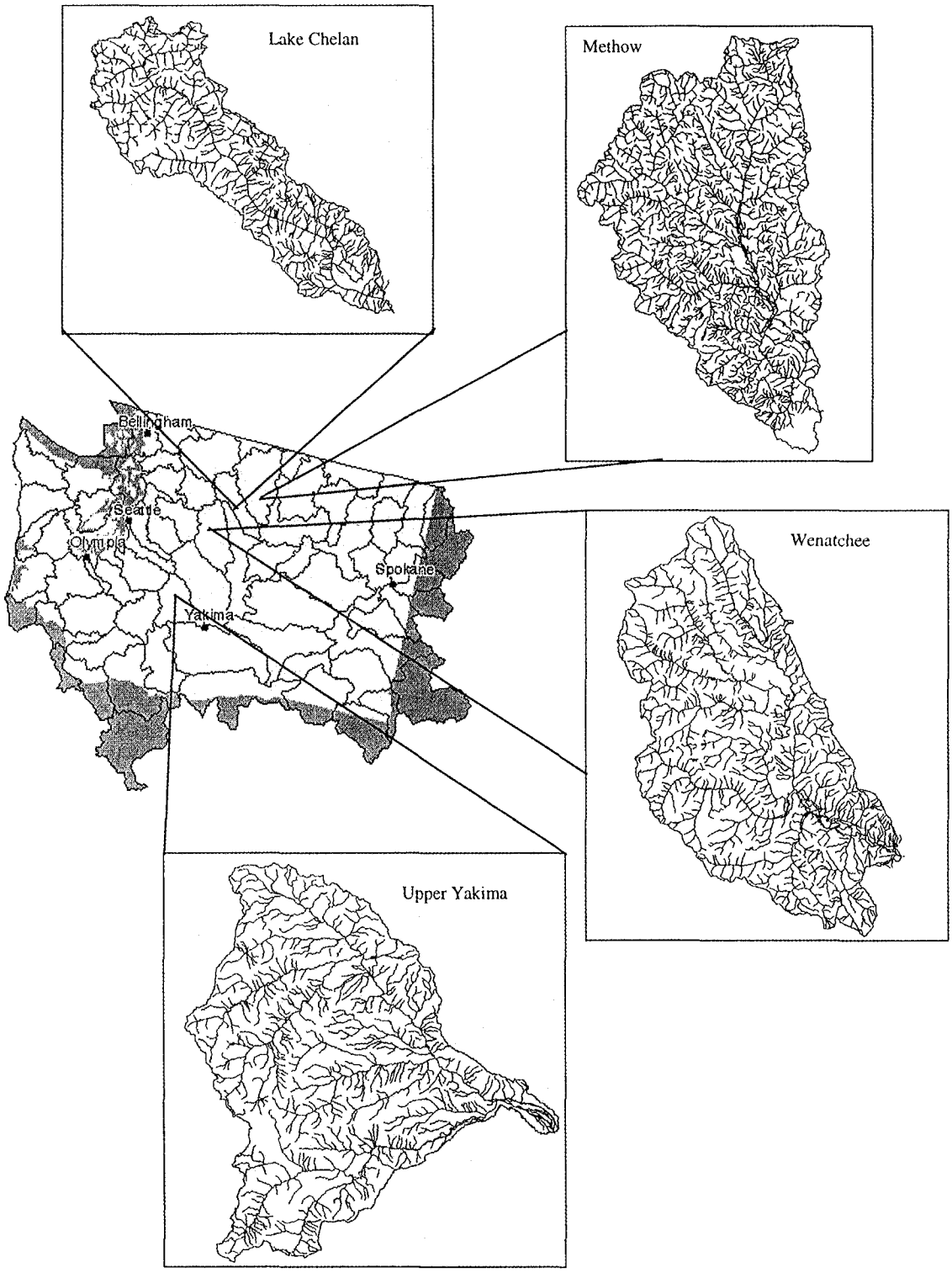

Figure 4. Location Map of Methow, Lake Chelan, Wenatchee and Upper Yakima River Basins. (Source of the state wide watershed boundaries: USEPA, 2001).

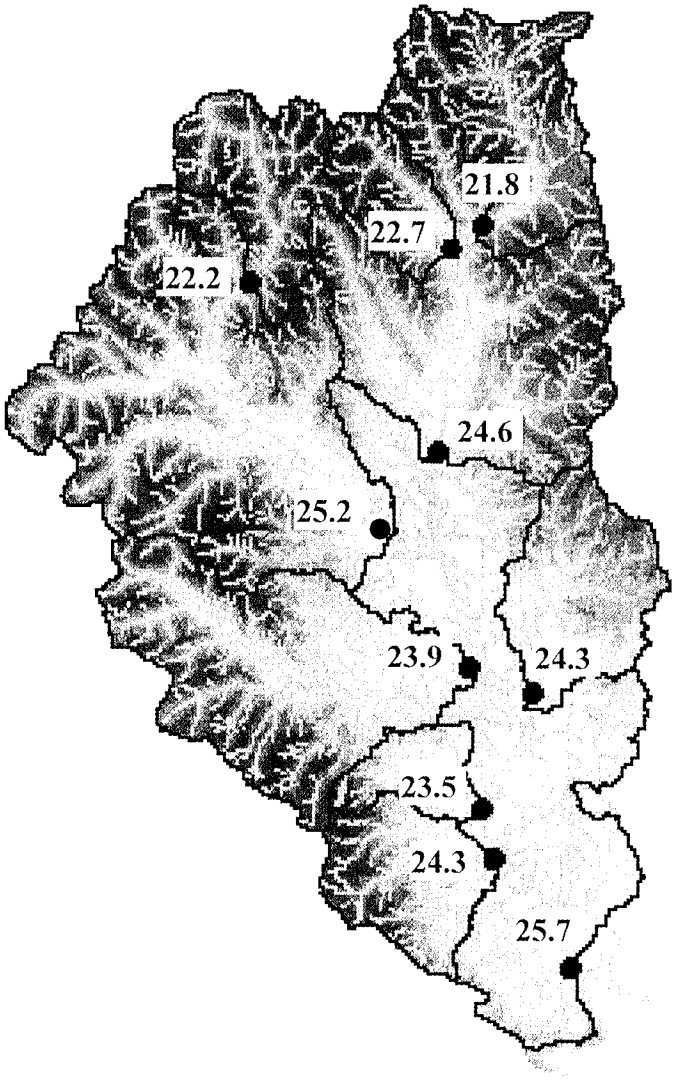

Figure 5. Maximum Water Temperature Results (°C) for the Methow River Basin.

the subbasins. Table 5 shows the ranked sensitivity coefficients for the Methow River (other results were similar). In these sensitivity analyses, LAI was the most sensitive parameter related to land use management. An increase of 1.6 to 1.8°C in simulated temperatures occurred for reduced LAI, as would be associated with immature or sparse vegetation. On the other hand, increases in LAI to over 10 (the nominal value was 7) had no effect on stream temperature, primarily because solar radiation is almost completely attenuated by canopies with LAI of 7, which corresponds to a fairly mature and dense forest. Reduction of tree height with subsequent heating of the stream by the increased solar radiation causes an increase in the estimated stream temperature up to 0.5°C (arguably the actual increase might be more, as LAI usually decreases with vegetation height, although it was kept constant here). Similar to LAI, any change in tree height above 30 m (more than 150 percent of the control run height of 20 m) resulted in minimal change as the radiation penetration to the stream is greatly affected. Buffer width was the third significant parameter but a buffer width beyond 30 m had only minimal effect on the stream temperature. It is emphasized that this result is applicable to vegetation typically present in the catchments studied, specifically coniferous forests with LAI in the general range 4 to 5 at the low end (for some stands of Lodge pole pine) to as much as 15 for some mature stands of Douglas Fir. For such vegetation, this conclusion is

Figure 6. Maximum Water Temperature Results (°C) for the Chelan River Basin.

quite robust. Bank canopy distance was the least sensitive parameter when compared with other parameters; increasing the distance beyond 10 m had only a minimal effect on stream temperature. This is because the geometric effect of the canopy on solar radiation attenuation, for a given solar azimuth, is not changed much by simply moving the vegetation away from the bank. It should be emphasized, however, that this model assumes that vegetation ends at the stream bank (i.e., there is no vegetation overhang). Were this considered, it is likely that removal of overhanging vegetation, by increasing bank-canopy distance, would substantially affect stream temperature. Overall, the results show that canopies close to the stream, with buffer widths of at least 30 m, play an important role in modulating the temperature of the stream.

SUMMARY AND CONCLUSIONS

The physically based GIS-STRTEMP stream temperature model was able to predict maximum stream temperatures during the critical summer low flow period for streams on both the east and west slopes of the Cascades. Additional simulations carried out over four east slope Cascade basins, which can experience relatively high maximum summer temperatures, illustrated the potential use of the method to evaluate combinations of natural factors and streamside vegetation management, which is of particular concern for water quality management. Stream orientation, as computed from digital topographic data, was important in determining maximum temperatures. Streams having a north-south orientation tended to be warmer than those with an east-west orientation. Of the factors related to streamside vegetation, LAI of the streamside vegetation had the greatest effect on

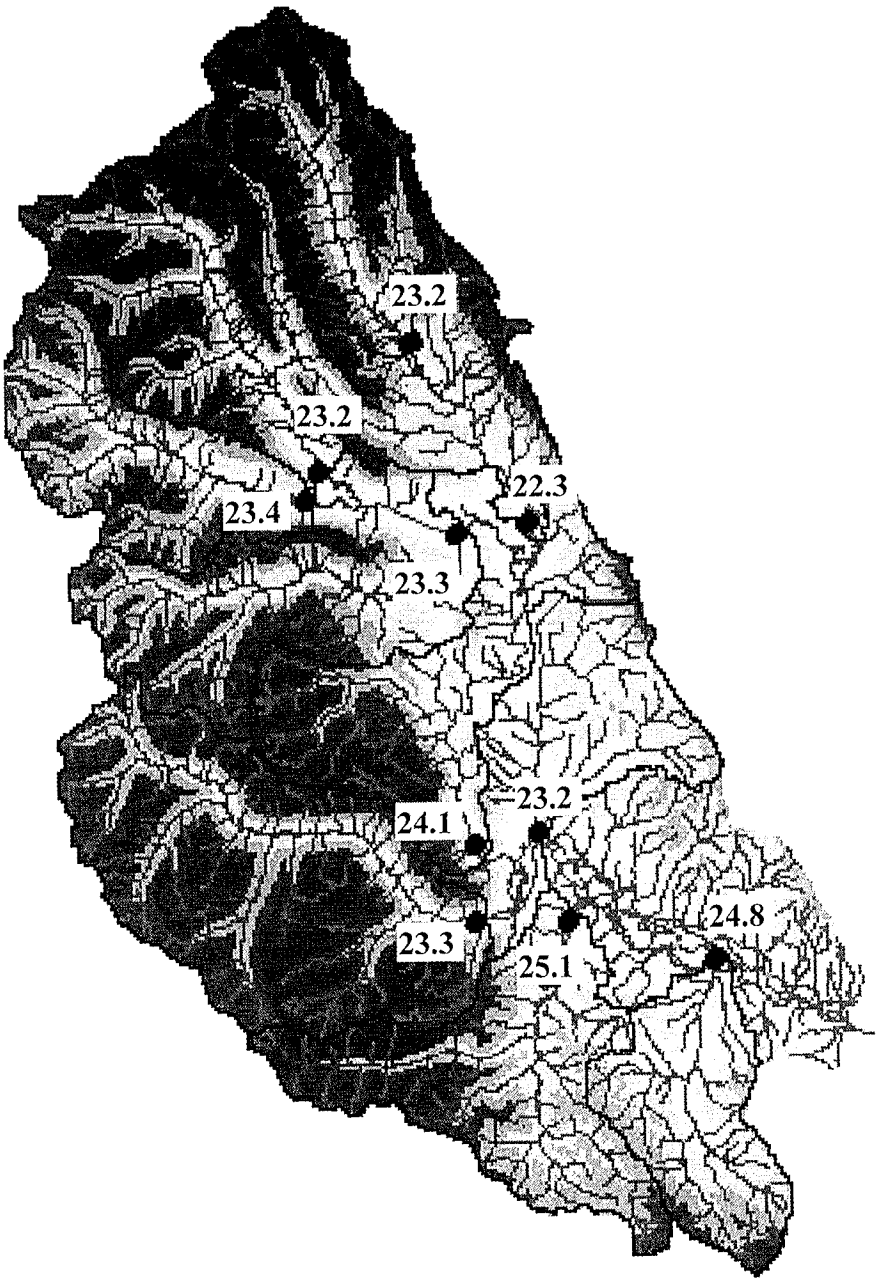

Figure 7. Maximum Water Temperature Results (°C) for the Wenatchee River Basin.

stream temperatures. Average tree height, which determines the shade and penetration of solar radiation in the basin, appeared to be the second most sensitive parameter followed by buffer width and bank/canopy distance. Buffer widths greater than about 30 m had only minimal effect on stream temperature, however. The largest stream temperature reductions were predicted for mature (high LAI) canopies close to the stream (i.e., within 10 m of the stream bank) and having width of about 30 m.

Among the limitations of this relatively simple model are that the stream azimuths and associated vegetation parameters (e.g., tree height and buffer width) are prescribed for the entire reach. Allowing specification of more general channel orientations (e.g., through use of multiple reaches) would enhance the model applicability for larger stream systems with changing buffers, but would complicate model implementation. Likewise, additional data on 7Q10 discharge, stream temperatures, and vegetation

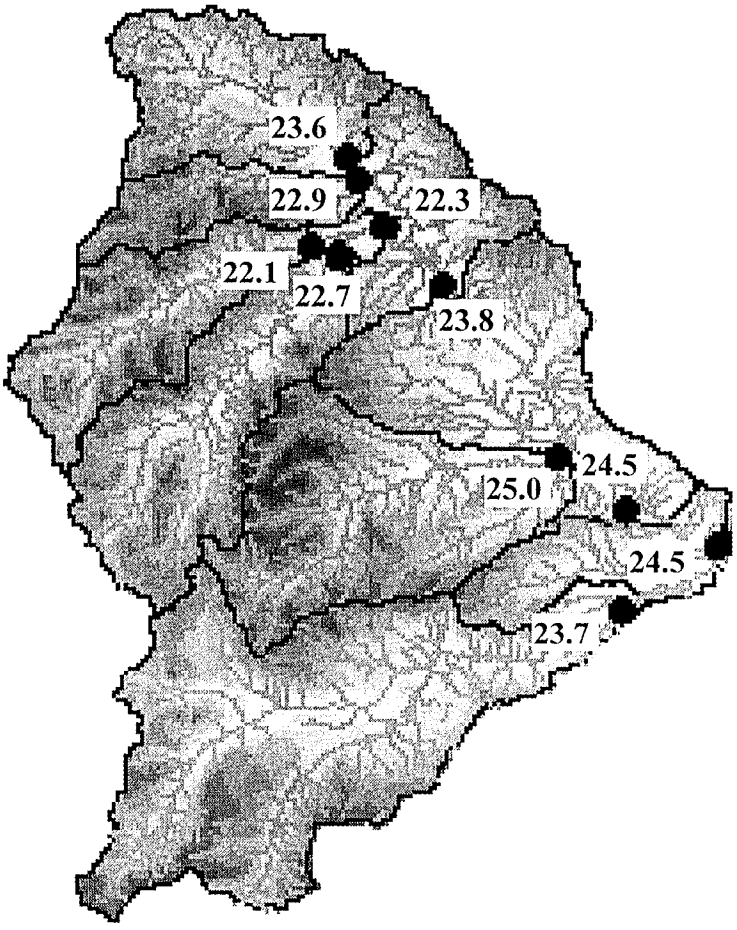

Figure 8. Maximum Water Temperature Results (°C) for the Upper Yakima River Basin.

parameters would allow a more general model implementation, but would, in the authors' view, detract from the applicability of the model over large areas. In any event, such data are not generally available. Furthermore, it was found that the upstream boundary condition, if chosen appropriately, did not significantly affect the predicted stream temperatures.

ACKNOWLEDGMENTS

The research reported in this paper was supported by Cooperative Agreement No. PNW 98-0514-1-CA and Joint Venture Agreement No. PNW 00-JV-11261927-522 between the U.S. Forest Service and the University of Washington.

LITERATURE CITED

Andradóttir, H. Ó and H.M. Nepf, 2000. Thermal Mediation by Littoral Wetlands and Impact on Lake Intrusion Depth. Water Resources Research, 36(3):725-735.

Bowen, I.S., 1926. The Ratio of Heat Losses by Conduction and by Evaporation From Any Water Surface. Physical Review 27:779-787.

Brosofske, K.D., J. Chen, R.J. Naiman, and J.F. Franklin, 1997. Harvesting Effects on Microclimatic Gradients From Small Streams to Uplands in Western Washington. Ecological Applications 7:1188-1200.

Brown, G.W., 1969. Predicting Temperatures of Small Streams. Water Resources Research 5:68-75.

Chapra, S.C., 1997. Surface Water-Quality Modeling. McGraw-Hill Series in Water Resources and Environmental Engineering, WCB/McGraw-Hill, New York, New York, 844 pp.

Daly, C., R.P. Neilson, and D.L. Phillips, 1994. A Statistical-Topographic Model for Mapping Climatological Precipitation Over Mountainous Terrain. Journal of Applied Meteorology 33:140-158.

Dubayah, R. and P.M. Rich, 1995. Topographic Solar Radiation Models for GIS. International Journal for Geographical Information Systems 9:405-419.

Helsel, D.R. and R.M. Hirsch, 1992. Statistical Methods in Water Resources. Studies in Environmental Science 49, Elsevier, New York, New York, 522 pp.

Hynes, H.B.N., 1970. The Ecology of Running Waters. University of Toronto Press, Toronto, Canada, 555 pp.

Jaske, R.T., 1965. Prediction of Columbia River Temperatures Downstream From Grand Coulee Dam for Wide Extremes of Flow and Weather Conditions. Pacific Northwest Laboratories, Battelle Memorial Institute, Richland, Washington, 19 pp.

Lowney, C.L., 2000. Stream Temperature Variation in Regulated Rivers: Evidence for a Spatial Pattern in Daily Minimum and Maximum Magnitudes. Water Resources Research 36(10):2947-2955.

Monteith, J.L. and M.H. Unsworth, 1990. Principles of Environmental Physics. Edward Arnold, London, United Kingdom, 291 pp.

Penman, H.L., 1948. Natural Evaporation From Open Water, Bare Soil and Grass. Proceedings of the Royal Society of London, A193:120-145.

Raphael, J.M., 1962. Prediction of Temperature in Rivers and Reservoirs. Journal of the Power Division, American Society of Civil Engineers, 88(PO2): 157-181.

Rich, P.M., W.A. Hetrick, and S.C. Saving, 1994. Modeling Topographic Influences on Solar Radiation: A Manual for the SOLARFLUX Model. Los Alamos National Laboratory Manual LA-12989-M, 29 pp.

Rishel, G.B., J.A. Lynch, and E.S. Corbett, 1982. Seasonal Stream Temperature Changes Following Harvesting. Journal of Environmental Quality 11:112-116.

Salo, E.O. and T. W. Cundy, 1987. Forestry and Fisheries Interactions. College of Forest Resources, Institute of Forest Resources, 467 pp.

Sansone, A.L. and D.P. Lettenmaier, 2001. A GIS-Based Temperature Model for the Prediction of Maximum Stream Temperatures in the Cascade Mountain Region. Water Resources Series Technical Report No. 168, University of Washington, 93 pp.

Sartoris, J.J., 1976. A *Mathematical Model for Predicting River* Temperatures – Application to the Green River Below Flaming Gorge Dam. U.S. Bureau of Reclamation Engineering and Research Center, Report REC-ERC-76-7, 28 pp.

Shuttleworth, W.J., 1993. Evaporation. *In:* Handbook of Hydrology, D.R. Maidment (Editor). McGraw-Hill, New York, New York, Chapter 4.

Sinokrat, B.A. and H.G. Stefan, 1993. Stream Temperature Dynamics: Measurement and Modeling. Water Resources Research 29:2299-2312.

Stedinger, J.R. and G.D. Tasker, 1985. Regional Hydrologic Analysis. 1. Ordinary, Weighted, and Generalized Least Squares Compared. Water Resources Research 21:1421-1432.

Sullivan, K., J. Tooley, K. Doughty, J.E. Caldwell, and P. Knudsen, 1990. Evaluation of Prediction Models and Characterization of Stream Temperature Regimes in Washington. Timber/Fish/Wildlife Rep. No. TFW-WQ3-90-006, Washington Department of Natural Resources, Olympia, Washington, 224 pp.

Tasker, G.D. and J.R. Stedinger, 1989. An Operational GLS Model for Hydrologic Regression. Journal of Hydrology 111:361-375.

Theurer, F.D., K.A. Voos, and W.J. Miller, 1984. Instream Water Temperature Model. Instream Flow Info. Paper No. 16, U.S. Department of Interior Fish and Wildlife Service FWS/OBS-84/15.

Thomas. D.M., and M.A. Benson, 1970. Generalization of Streamflow Characteristics From Drainage-Basin Characteristics, U.S. Geological Survey Professional Paper 1975.

USEPA (U.S. Environmental Protection Agency), 2001. Surf Your Watershed: Washington. *Available at* http://cfpub.epa.gov/surf/state.cfm?statepostal=WA. *Accessed in* October 2001.

TABLE 4. Simulated Minimum, Maximum, and Average Temperatures for Methow, Lake Chelan, Wenatchee, and Upper Yakima Basins.

Subbasin	Average	Minimum	Maximum
Methow Basin			
1	19.6	16.9	21.8
2	20.1	17.1	22.7
3	19.6	16.6	22.2
4	23.1	20.4	25.2
5	22.7	20.3	24.6
6	21.5	18.6	23.9
7	22.0	19.3	24.3
8	21.4	18.2	23.5
9	21.5	18.0	24.3
10	22.5	20.4	25.7
Lake Chelan Basin			
1	19.6	16.5	22.5
2	19.7	16.5	21.8
3	20.1	17.2	22.2
4	20.1	17.1	23.1
5	21.7	18.3	24.1
6	18.1	14.8	21.1
7	21.8	18.4	25.1
8	20.2	16.9	22.6
9	22.1	20.1	23.6
10	22.7	20.3	24.2
WenatcheeBasin			
1	20.5	17.2	23.2
2	20.9	18.1	23.2
3	20.8	17.4	23.4
4	20.3	17.9	22.3
5	21.3	18.4	23.3
6	22.0	19.5	24.1
7	21.0	18.3	23.3
8	21.2	18.4	23.2
9	22.7	19.7	25.1
10	22.8	19.9	24.8
Upper Yakima Basin			
1	21.4	18.3	23.6
2	20.2	17.0	22.9
3	20.5	17.6	22.1
4	21.0	18.3	22.7
5	20.7	17.8	22.3
6	21.7	18.9	23.8
7	21.9	18.5	25.0
8	21.6	18.6	23.7
9	22.6	20.0	24.5
10	22.3	19.6	24.5

TABLE 5. Sensitivity Analysis Results for the Methow River Basin.

Parameter (estimate)	Subbasin 1		Subbasin 2		Subbasin 3	
	Sr (percent)	*S*(°C)	*Sr* (percent)	*S*(°C)	*Sr* (percent)	*S*(°C)
LAI (4)	11.59	1.63	10.68	1.75	12.05	1.88
Tree Height (10)	9.32	0.48	8.61	0.52	9.66	0.55
LAI (2)	5.59	0.97	5.18	1.04	5.84	1.12
Tree Height (0)	3.03	0.24	2.82	0.25	3.18	0.27
Buffer Width (15)	-3.21	-0.33	-2.95	-0.35	-3.34	-0.38
Buffer Width (30)	-3.21	-0.17	-2.95	-0.18	-3.34	-0.19
Buffer Width (50)	-3.21	-0.10	-2.95	-0.11	-3.34	-0.11
Bank Canopy Dist. (50)	-3.29	-0.10	-3.06	-0.11	-3.45	-0.11
Tree Height (200)	-3.98	-0.03	-3.70	-0.03	-4.18	-0.03
Bank Canopy Dist. (10)	-4.70	-0.61	-4.32	-0.65	-4.79	-0.69
LAI (17)	-7.73	-0.50	-7.10	-0.53	-8.02	-0.57

Note: $Absolute.sensitivity(S) = \frac{O_2 - O_1}{P_2 - P_1}$ $\quad Relative.sensitivity(Sr) = \frac{O_2 - O_1}{P_2 - P_1} \cdot \frac{P}{O}$

where Parameter (P) is given by $\frac{P_1 + P_2}{2}$; Output (O) is given by $\frac{O_1 + O_2}{2}$

Here, P1 and O1 represent the reference parameter and output values and P2 and O2 represent the changed values of parameter and the resulting output.